

Pigeon-inspired optimization and extreme learning machine via wavelet packet analysis for predicting bulk commodity futures prices

Feng JIANG^{1*}, Jiaqi HE¹ & Zhigang ZENG^{2*}

¹*School of Statistics and Mathematics, Zhongnan University of Economics and Law, Wuhan 430073, China;*

²*School of Automation, Huazhong University of Science and Technology, Wuhan 430074, China*

Received 15 August 2018/Accepted 30 November 2018/Published online 31 May 2019

Abstract In this paper, a hybrid approach consisting of pigeon-inspired optimization (PIO) and extreme learning machine (ELM) based on wavelet packet analysis (WPA) is presented for predicting bulk commodity futures prices. Firstly, WPA is applied to decompose the original futures prices into a set of lower-frequency subseries. Secondly, the PIO algorithm is used to optimize the parameters of ELM and then the optimized ELM is utilized to forecast the subseries. Finally, we adopt the hybrid method to calculate the final forecasting outcomes of futures prices. In order to further test the predictive ability of the hybrid forecasting model on bulk commodity futures prices, we use the prices of West Texas Intermediate crude oil futures and Chicago Board of Trade soybean futures to make one-step, two-step and four-step ahead predictions. In comparison with complete ensemble empirical mode decomposition with adaptive noise, empirical mode decomposition and singular spectrum analysis, WPA is the most suitable for decomposing bulk commodity futures prices. The experimental outcomes show that the hybrid WPA-PIO-ELM model has better performance on horizontal precision, directional precision and robustness.

Keywords wavelet packet analysis, extreme learning machine, pigeon-inspired optimization, bulk commodity futures price prediction, directional precision

Citation Jiang F, He J Q, Zeng Z G. Pigeon-inspired optimization and extreme learning machine via wavelet packet analysis for predicting bulk commodity futures prices. *Sci China Inf Sci*, 2019, 62(7): 070204, <https://doi.org/10.1007/s11432-018-9714-5>

1 Introduction

Bulk commodity futures are indispensable connections between commodity and futures markets, and the prices of bulk commodity futures are important references for both commodity and futures traders. Bulk commodity futures prices also reflect changes in the global economy. Owing to the influence of political factors, scientific development, economic globalization and other uncertain elements, the prices of bulk commodity futures have experienced dramatic shifts. As a result, the accurate prediction of bulk commodity futures prices has become increasingly difficult.

Traditional statistical approaches, such as Grey-Markov model [1] and autoregressive integrated moving average (ARIMA) [2, 3] have been utilized to predict futures prices. In recent years, intelligent approaches [4–7], such as artificial neural network (ANN) [8–10], support vector machine (SVM) [11–13], difference algorithm (DE) [14], and pigeon-inspired optimization (PIO) [15], have better predicting precision for big data. Chen et al. [16] utilized the ANN to forecast gold futures prices. Comparing with

* Corresponding author (email: fjiang78@163.com, zgzen@hust.edu.cn)

the approach of ARIMA, ANN is more accurate for predicting the prices of gold futures. Duan et al. [17] utilized PIO to control unmanned air vehicles. The empirical analysis indicates that the PIO algorithm has better optimizing performance than DE and other optimization algorithms. Therefore, with the rapid development of artificial intelligence, neural networks have become more suitable for forecasting the prices of futures and other types of time series, such as electricity prices and air quality index.

In order to resolve the high volatility of time series, empirical mode decomposition (EMD) [18], ensemble empirical mode decomposition (EEMD) [19], wavelet packet analysis (WPA) [20] and other decomposition algorithms [21, 22] have caught the eyes of scholars. Wang et al. [23] combined singular spectrum analysis (SSA), K-means and extreme learning machine (ELM) together and utilized the SSA-K-means-ELM model to predict the prices of corn, gold and crude oil futures. The hybrid SSA-K-means-ELM approach has great advantages on both horizontal estimation and directional estimation. Lu [24] adopted a hybrid model of EMD and radial basis function neural network (RBF) to predict the stock index futures accurately. EMD can decompose the initial data into a set of intrinsic mode functions and enhance the forecasting precision of RBF. Wang et al. [25] used a hybrid model of SSA and neural networks to forecast the prices of corn futures, West Texas Intermediate (WTI) crude oil futures and gold futures. SSA can reduce the prediction difficulty of the original futures series. By decomposing the series of initial signals, the artificial intelligence approaches can forecast the subseries more accurately.

By comparing different decomposition methods, we propose a hybrid approach of PIO and ELM based on WPA to predict the prices of bulk commodity futures more accurately. We also adopt PIO to optimize the initial weights and thresholds of ELM. The remainder of this paper is organized as bellow. Section 2 introduces the relevant methodologies utilized in this paper. Section 3 presents the empirical analysis outcomes and the comparative results of the hybrid forecasting model. Horizontal precision, directional precision and robustness are also examined by using statistical indicators and statistical tests. A conclusion of this paper is given in Section 4.

2 Related methodologies

In this section, we introduce the methodologies of WPA, PIO and ELM and then build a hybrid model of PIO and ELM based on WPA to forecast bulk commodity futures prices.

2.1 Wavelet packet analysis

WPA is an improved decomposition method based on wavelet analysis (WA), which can continuously decompose both low-frequency and high-frequency components of the original signals. With respect to decomposition and de-noising, WPA is more effective than WA and it can decompose non-stationary, nonlinear and complicated series into a set of lower-frequency subseries. WPA has been widely used in the fields of industry, environmental analysis, economics and finance. The wavelet function is shown as follows:

$$\begin{cases} \mu_0(t) = \sqrt{2} \sum_{k \in Z} h(k) \mu_0(2t - k), \\ \mu_1(t) = \sqrt{2} \sum_{k \in Z} g(k) \mu_0(2t - k). \end{cases} \quad (1)$$

Here $h(k)$ and $g(k)$ represent the low-pass and high-pass filtering functions respectively, and $g(k) = (-1)^k h(1 - k)$. The wavelet basis function $\varphi(t)$ and the scaling function $\psi(t)$ satisfy $\mu_0(t) = \varphi(t)$ and $\mu_1(t) = \psi(t)$.

The wavelet function satisfies a double scale function, which is denoted as follows:

$$\begin{cases} \mu_{2n}(t) = \sqrt{2} \sum_{k \in Z} h(k) \mu_n(2t - k), \\ \mu_{2n+1}(t) = \sqrt{2} \sum_{k \in Z} g(k) \mu_n(2t - k). \end{cases} \quad (2)$$

The decomposition algorithm is defined as follows:

$$\begin{cases} d_j^{2n}(k) = \sum_{t \in Z} h(t - 2k)d_{j+1}^n(t), \\ d_j^{2n+1}(k) = \sum_{t \in Z} g(t - 2k)d_{j+1}^n(t), \end{cases} \quad (3)$$

where d_j^{2n} and d_j^{2n+1} are the two decomposition coefficients.

The reconstruction algorithm is displayed as follows:

$$d_{j+1}^n(k) = \sum_{t \in Z} h(k - 2t)d_j^{2n}(t) + \sum_{t \in Z} g(k - 2t)d_j^{2n+1}(t). \quad (4)$$

Here $d_{j+1}^n(k)$ represents a reconstructed series of the initial signal.

2.2 Extreme learning machine

ELM belongs to a type of single hidden layer intelligent neural network proposed by Huang et al. [26]. ELM has excellent performance on adaptive ability, generalization ability and nonlinear mapping ability. In terms of training speed, ELM is much faster than the traditional RBF. The weights of hidden layer are obtained by the least square procedure. ELM is both simple and efficient and its initial weights and thresholds are important parameters, which are indispensable for the prediction outcomes. The algorithm flow of ELM is shown as follows.

Step 1. The weight and bias vectors are defined as follows:

$$w = (w_1, w_2, \dots, w_l)', \quad b = (b_1, b_2, \dots, b_l)'. \quad (5)$$

Step 2. Based on the activation function of the hidden layer $f(x)$, the output of the hidden layer H is presented as follows:

$$H = \begin{pmatrix} f(w_1 \cdot x_1 + b_1) & f(w_2 \cdot x_1 + b_2) & \cdots & f(w_l \cdot x_1 + b_l) \\ f(w_1 \cdot x_2 + b_1) & f(w_2 \cdot x_2 + b_2) & \cdots & f(w_l \cdot x_2 + b_l) \\ \vdots & \vdots & & \vdots \\ f(w_1 \cdot x_Q + b_1) & f(w_2 \cdot x_Q + b_2) & \cdots & f(w_l \cdot x_Q + b_l) \end{pmatrix}. \quad (6)$$

Step 3. By calculating the weights of the output layer $\hat{\beta}$ ($\hat{\beta} = H^+T'$), the final outcome of ELM is denoted as follows:

$$T = \begin{pmatrix} T_1 \\ T_2 \\ \vdots \\ T_Q \end{pmatrix}', \quad t_j = \begin{pmatrix} t_{1j} \\ t_{2j} \\ \vdots \\ t_{mj} \end{pmatrix} = \begin{pmatrix} \sum_{i=1}^l \beta_{i1}f(w_i x_j + b_i) \\ \sum_{i=1}^l \beta_{i2}f(w_i x_j + b_i) \\ \vdots \\ \sum_{i=1}^l \beta_{im}f(w_i x_j + b_i) \end{pmatrix}. \quad (7)$$

2.3 Pigeon-inspired optimization

PIO is a novel swarm optimization algorithm that was proposed by Duan et al. [27]. The PIO algorithm imitates the behaviors of pigeons in finding the location of their homes according to different navigation tools. In order to build a mathematical model, the map and compass operator and the landmark operator are applied in PIO. The optimization process has two indispensable elements, the position vector and the velocity vector. Their update approaches are shown as Eqs. (8) and (9), which are based on the map and compass operator at first.

$$V_j^l = V_j^{l-1} \cdot e^{-Rl} + r \cdot (X_{gbest} - X_j^{l-1}), \quad (8)$$

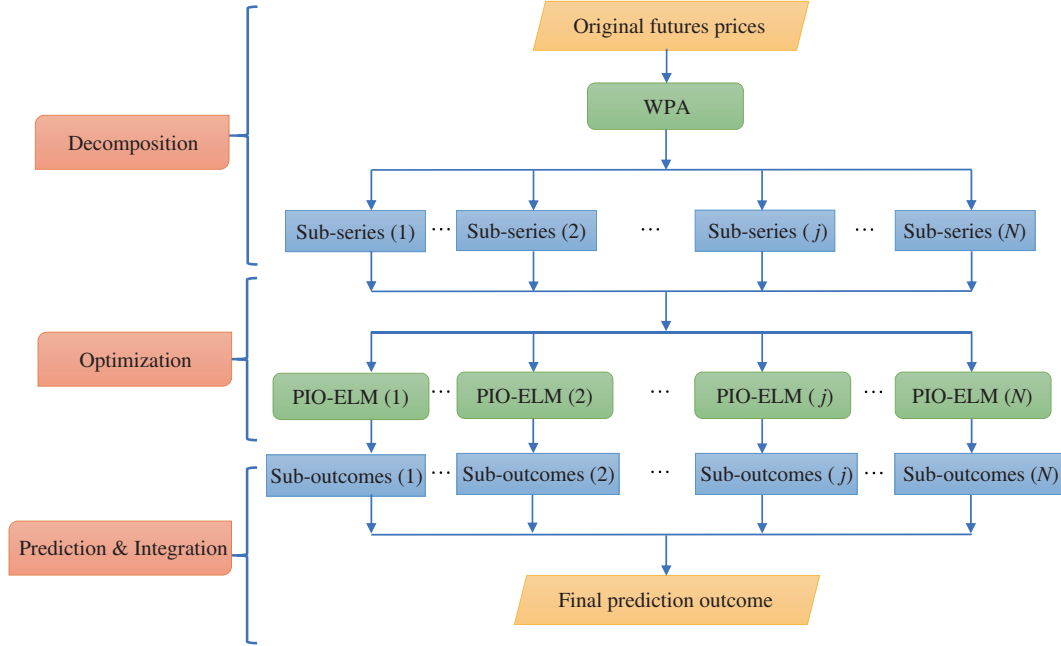


Figure 1 (Color online) Learning framework of the hybrid model.

$$X_j^l = X_j^{l-1} + V_j^l, \quad (9)$$

where V_j^l is the velocity vector, j and l denote the j -th pigeon and the l -th iteration respectively, X_j^l represents the position vector, X_{gbest} is the global best location in the current iteration, R denotes the map and compass coefficient and r is a random number between 0 and 1. When the number of iterations reaches a specified value, the optimization process based on the map and compass operator stops. In order to make pigeons fly close to their homes, another update approach of the position vector based on the landmark operator is defined as bellow. When implementing the landmark operator, the number of pigeons is reduced by half in each iterative process.

$$X_{\text{center}}^l = \frac{\sum X_j^l \cdot f(X_j^l)}{N_p \sum f(X_j^l)}, \quad (10)$$

$$X_j^l = X_j^{l-1} + r \cdot (X_{\text{center}}^l - X_j^{l-1}). \quad (11)$$

Here $f(\cdot)$ is the fitness function, X_{center}^l represents the current center of pigeons, and N_p is defined as

$$N_p^l = N_p^{l-1} / 2. \quad (12)$$

When the update process achieves the maximum number of iterations, the PIO algorithm stops and the location of the global optimal point is the final output of PIO.

2.4 Hybrid WPA-PIO-ELM learning approach

A hybrid approach of PIO and ELM based on WPA is proposed to predict futures prices of bulk commodities in this paper. As a decomposition method, WPA is used to decompose the original signals into a set of subseries. The PIO algorithm can find the global optimum according to the map and compass operator and the landmark operator. We adopt PIO to optimize the initial weights and thresholds of ELM, and the hybrid PIO-ELM approach is employed to forecast the subseries of the original bulk commodity futures prices. The final outcomes are calculated by the hybrid method. The learning framework and pseudo code of the hybrid WPA-PIO-ELM model are displayed in Figure 1 and Algorithm 1, respectively.

Algorithm 1 Hybrid WPA-PIO-ELM

```

1: Utilize WPA to decompose the original series into a set of subseries;
2: Input the subseries, build an ELM model, set the initial weights and thresholds of ELM as the optimization objects
   ( $X$ ), and set the prediction error as the fitness function of PIO  $f(x)$ ;
3: Initialize the parameters of the PIO algorithm, including the number of pigeons ( $N$ ), the dimension ( $D$ ) and the changing
   boundary  $[m, n]$  of the searching room, the map and compass coefficient ( $R$ ), the maximum number of iterations affected
   by the two operators ( $N_{O_1}, N_{O_2}$ ) in PIO and a random velocity ( $V_j$ ) and location ( $X_j$ ) of every pigeon;
4: while  $l \leq N_{O_1}$  do
5:   for each pigeon do
6:     Update their velocities and locations by Eqs. (8) and (9) and calculate their fitness values;
7:   end for
8:   Update the location of the global best pigeon  $X_{\text{gbest}}$ ;
9: end while
10: while  $N_{O_1} + 1 \leq l \leq N_{O_2}$  do
11:   for each pigeon do
12:     Update their velocities and locations by Eqs. (10), (11) and (12) and calculate their fitness values;
13:   end for
14:   Update the location of the global best pigeon  $X_{\text{gbest}}$ ;
15: end while
16: return  $X_{\text{gbest}}$ ;
17: Set  $X_{\text{gbest}}$  as the initial weights and thresholds of ELM and utilize the improved ELM to make predictions.

```

3 Empirical analysis

In this section, the hybrid WPA-PIO-ELM model is used to make one-step, two-step and four-step ahead predictions of the prices WTI crude oil futures and Chicago Board of Trade (CBOT) soybean futures prices. Error analysis, statistical tests, robustness analysis and comparative analysis of the proposed model are then discussed respectively.

3.1 Data description and statistical evaluation criteria

In this subsection, we introduce the data description of WTI crude oil futures and CBOT soybean futures. Then we describe the statistical indicators and statistical tests for evaluating the forecasting performance.

3.1.1 Data description

The data in this paper comprises the prices of WTI crude oil futures of New York commodity exchange and CBOT soybean futures of Chicago commodity futures exchange, which are obtained from US Energy Information Administration and Wind database. As types of energy and agricultural commodities, crude oil and soybean futures can represent bulk commodity futures. There are a total of 8864 market trading days of WTI crude oil futures prices from April 4th, 1983 to July 31st, 2018 and 9025 days of CBOT soybean futures prices from January 3rd, 1983 to July 31st, 2018. The futures prices are displayed in Figures 2 and 3. And the prices of the last three years are set as testing samples and the other samples are set as training sets.

3.1.2 Statistical evaluation criteria

Statistical indicators and statistical tests are utilized to evaluate the forecasting performance of the proposed model. Six statistical indicators are selected to calculate the forecasting errors, which are mean absolute percentage error (MAPE), root mean square error (RMSE), normalized root mean square error (NRMSE), Theil's coefficient (TIC), index of agreement (IA) and direction statistics (Ds). The six mathematical formulae are shown in Table 1.

Here $H(t)$ indicates the actual value of the futures price, $\hat{H}(t)$ indicates the forecasted value of the futures price, \bar{H} is the mean value of real futures prices, t represents the t -th testing sample and T is the total number of testing samples. Ds is a statistical indicator which can be used to determine whether the predicted results have the same change direction as the actual values. If the value of $(H(t) - H(t-1))(\hat{H}(t) - H(t-1))$ is greater than 0, $\gamma(t)=1$; otherwise, $\gamma(t)=0$.

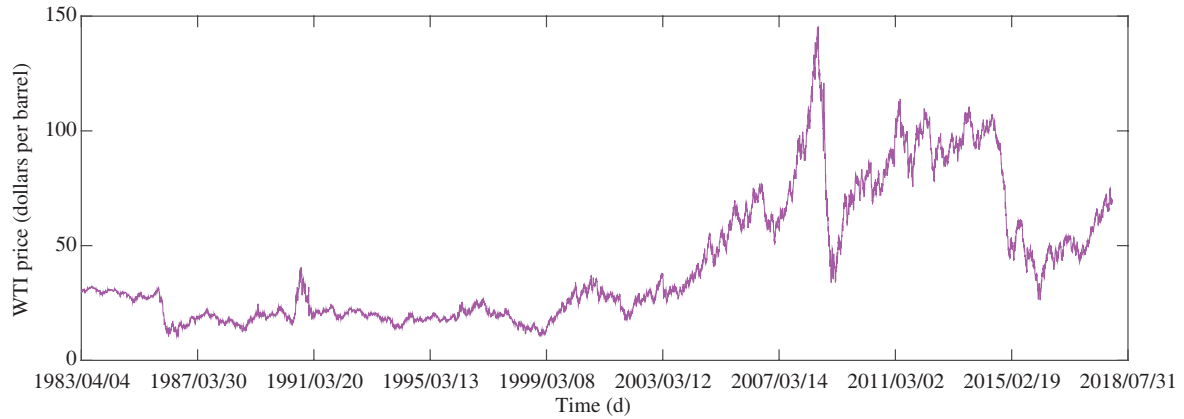


Figure 2 (Color online) Futures prices of WTI crude oil.

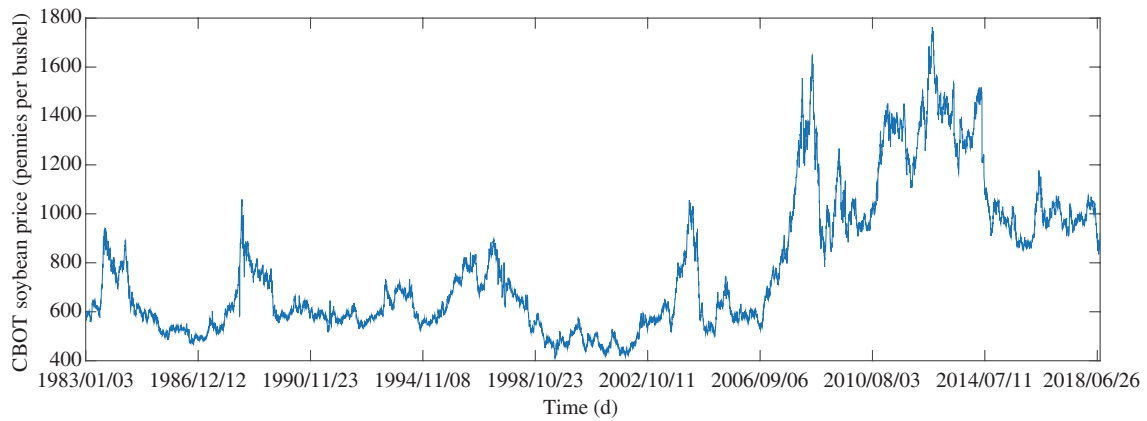


Figure 3 (Color online) Futures prices of CBOT soybean.

Table 1 Calculation formulae of statistical indicators

Statistical indicator	Calculation method
MAPE	$MAPE = \frac{1}{T} \sum_{t=1}^T \left \frac{\hat{H}(t) - H(t)}{H(t)} \right \times 100\%$
RMSE	$RMSE = \sqrt{\frac{1}{T} \sum_{t=1}^T (\hat{H}(t) - H(t))^2}$
NRMSE	$NRMSE = \frac{100}{H} \sqrt{\frac{1}{T} \sum_{t=1}^T (\hat{H}(t) - H(t))^2} \times 100\%$
TIC	$TIC = \frac{\sqrt{\frac{1}{T} \sum_{t=1}^T (\hat{H}(t) - H(t))^2}}{\sqrt{\frac{1}{T} \sum_{t=1}^T \hat{H}(t)^2 + \sqrt{\frac{1}{T} \sum_{t=1}^T H(t)^2}}}$
IA	$IA = 1 - \frac{\sum_{t=1}^T (\hat{H}(t) - H(t))^2}{\sum_{t=1}^T (\hat{H}(t) - \bar{H} + H(t) - \bar{H})^2}$
Ds	$Ds = \frac{1}{T} \sum_{t=2}^T \gamma(t) \times 100\%$

The first five indicators are applied to measure horizontal errors and the Ds indicator is applied to calculate directional errors. For a better predicting model, the values of MAPE, RMSE, NRMSE and TIC should be close to 0, and the values of IA and Ds should be equivalent to 1.

For further evaluating the prediction performance of the models, two statistical tests, Diebold-Mariano (DM) and Pesaran-Timmermann (PT) tests are utilized to analyze the horizontal and directional predictive ability from a statistical perspective [28,29]. The alternative hypotheses of the two tests are that the forecasting performance of the benchmark model is better than the tested models and the tested model can accurately predict the change direction respectively. Based on the results of statistical indicators and tests, we can make a comprehensive evaluation of the proposed model.

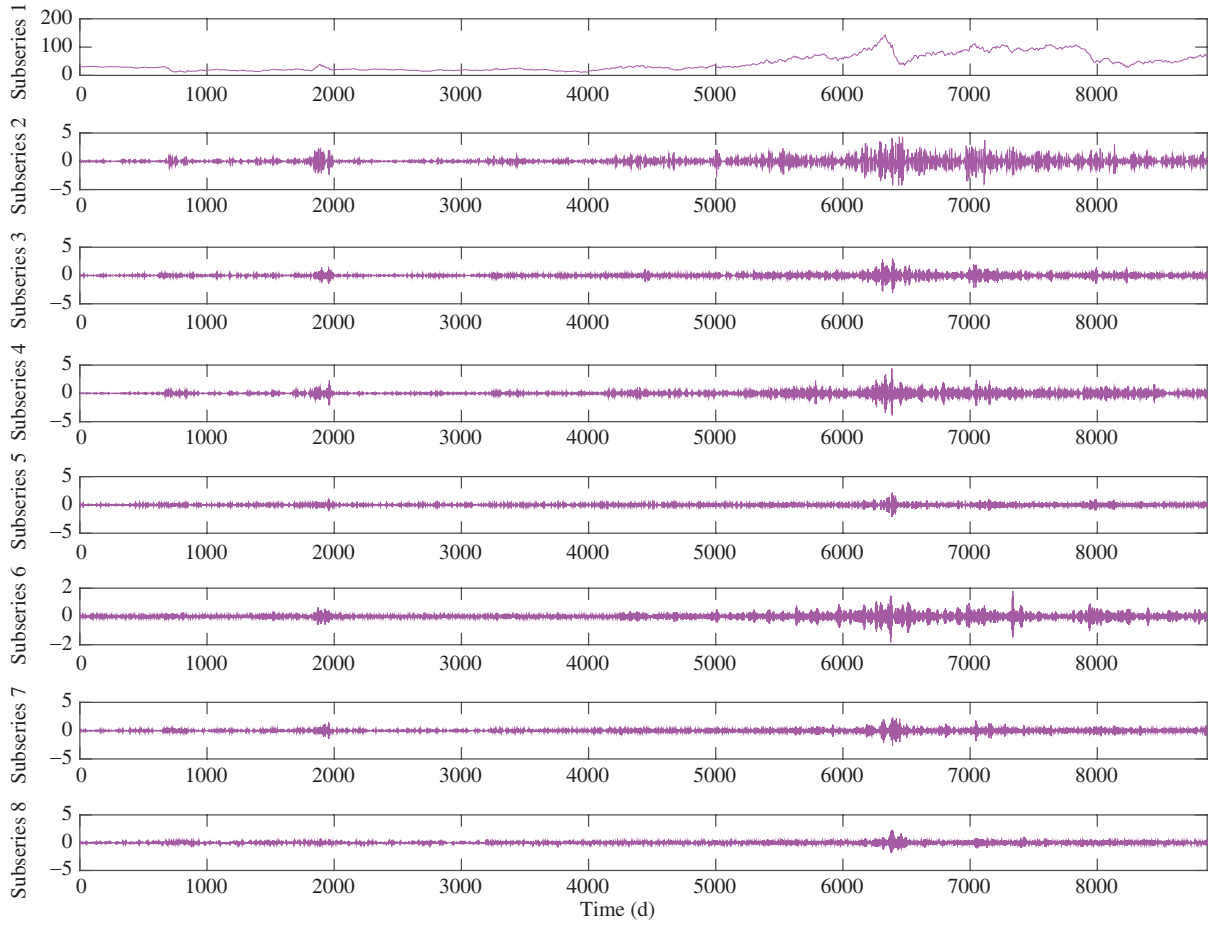


Figure 4 (Color online) Decomposition of WTI crude oil futures prices.

3.2 Comparative analysis

In this subsection, two types of bulk commodity futures are utilized to test the forecasting ability of the hybrid model. In order to verify the prediction performance, error analysis results and statistical test results are presented respectively.

3.2.1 Comparative analysis of WTI crude oil futures forecasting

Complete ensemble empirical mode decomposition with adaptive noise (CEEMDAN) [30] is an effective improvement of the original EMD algorithm. For comparing the predictive effects of the proposed model, CEEMDAN-PIO-ELM, PIO-ELM, ELM, least square support vector machine (LSSVM), generalized regression neural network (GRNN) and back propagation neural network (BPNN) are assigned as comparison models to forecast the prices of bulk commodity futures. For testing the predictive capability of the forecasting approaches, one-step, two-step and four-step ahead predictions are utilized to forecast the bulk commodity futures prices. For n -step ahead prediction,

$$\hat{y}_{t+n} = g(y_{t-h}, \dots, y_{t-1}, y_t), \quad t = 1, 2, \dots, T. \quad (13)$$

Here y_t represents the original series at the time of t , \hat{y}_{t+n} represents the predicted values of the original price at the time of $(t+n)$, and the n -step ahead prediction utilizes the first h prices to forecast the $(t+n)$ -th futures price. In this paper, seven data is set as a cycle to predict the futures prices in the following time.

We first adopt a three-layer WPA to decompose the prices of WTI crude oil futures into a set of subseries. Figure 4 illustrates the decomposition subseries of WTI crude oil futures. And Figures 5–10

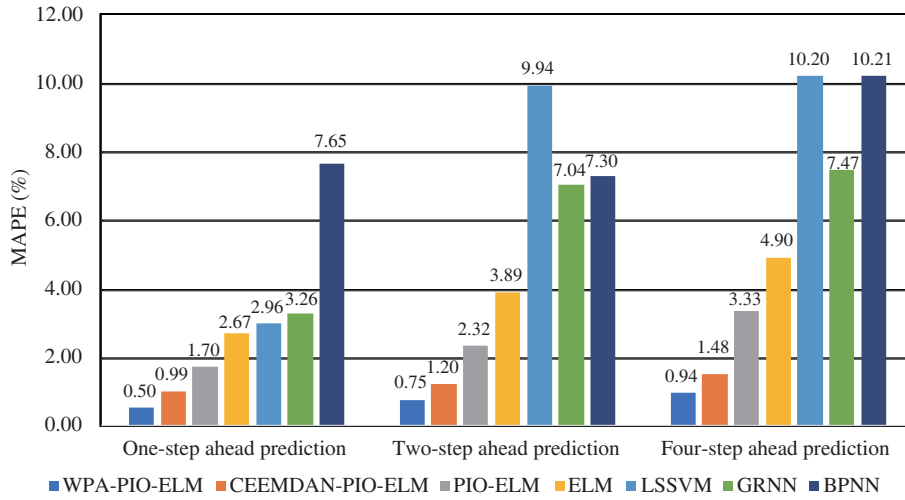


Figure 5 (Color online) MAPE of WTI crude oil futures prediction.

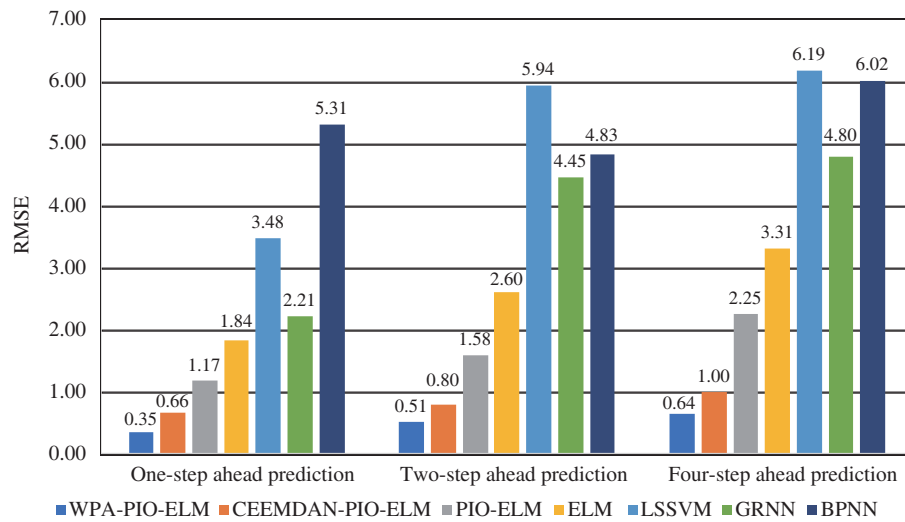


Figure 6 (Color online) RMSE of WTI crude oil futures prediction.

display the errors of the seven forecasting models of one-step, two-step and four-step ahead predictions. Based on the outcomes of error analysis, we can conclude that: (1) For each type of prediction, the hybrid-forecasting model proposed in this paper has the fewest errors for all six statistical indicators. This hybrid WPA-PIO-ELM model has the best predictive performance on the horizontal and directional estimation. The RMSE values of the proposed hybrid-forecasting model for one-step, two-step and four-step ahead predictions are 0.35, 0.51 and 0.64 respectively, which are nearly half of the values of CEEMDAN-PIO-ELM. The values for the directional precision of the WPA-PIO-ELM are 90.40%, 87.57% and 81.35%, which are the highest among the whole models. The proposed model has the best predictive accuracy for commodity futures prices. (2) The errors of CEEMDAN-PIO-ELM are all higher than those of WPA-PIO-ELM, which indicates that WPA is more suitable than CEEMDAN for decomposing commodity futures prices. (3) Comparing the outcomes of PIO-ELM and ELM, PIO-ELM can reduce the forecasting errors of MAPE and RMSE by more than 30%. However, for both models, the values of D_s indicator are nearly the same. It shows that PIO-ELM can effectively optimize the parameters of ELM and improve its horizontal predictive accuracy. (4) Among the four single models, the forecasting precision of ELM is much higher than that of the other three models. And BPNN has the poorest predictive performance among the whole forecasting models. For the three types of prediction, the capabilities of GRNN and LSSVM are similar to each other.

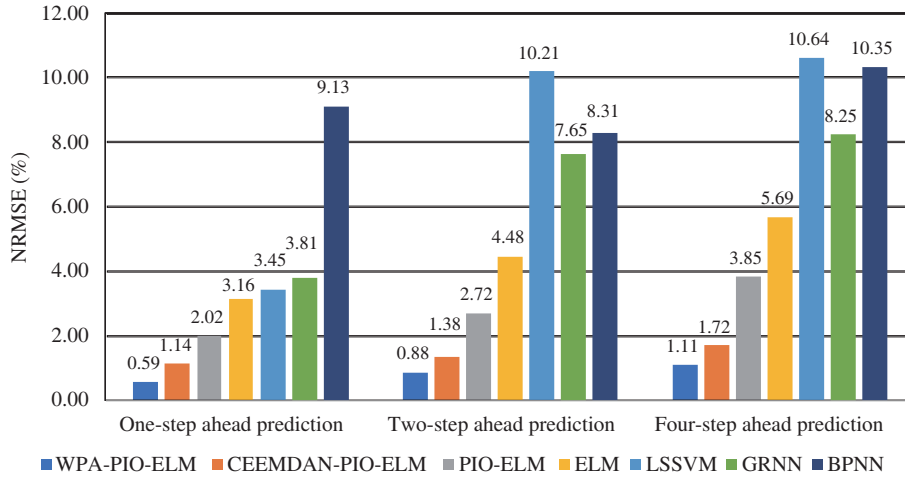


Figure 7 (Color online) NRMSE of WTI crude oil futures prediction.

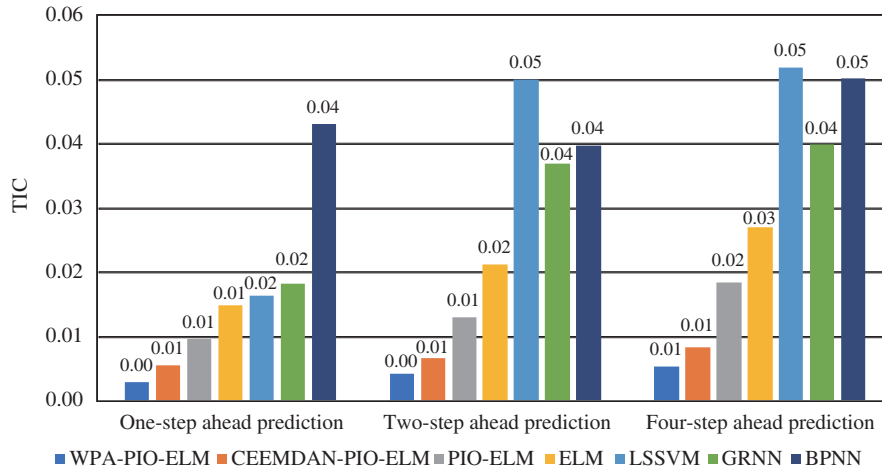


Figure 8 (Color online) TIC of WTI crude oil futures prediction.

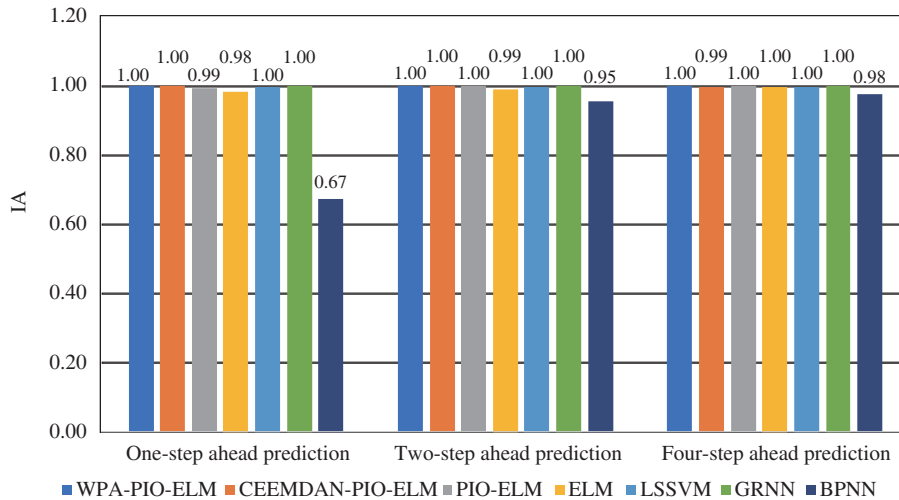


Figure 9 (Color online) IA of WTI crude oil futures prediction.

Tables 2–5 display the results of DM tests for one-step, two-step and four-step ahead predictions and the values outside the brackets are the values of DM statistical indicators and the values inside the brackets are p -values. DM test can examine whether the benchmark models are more accurate than the

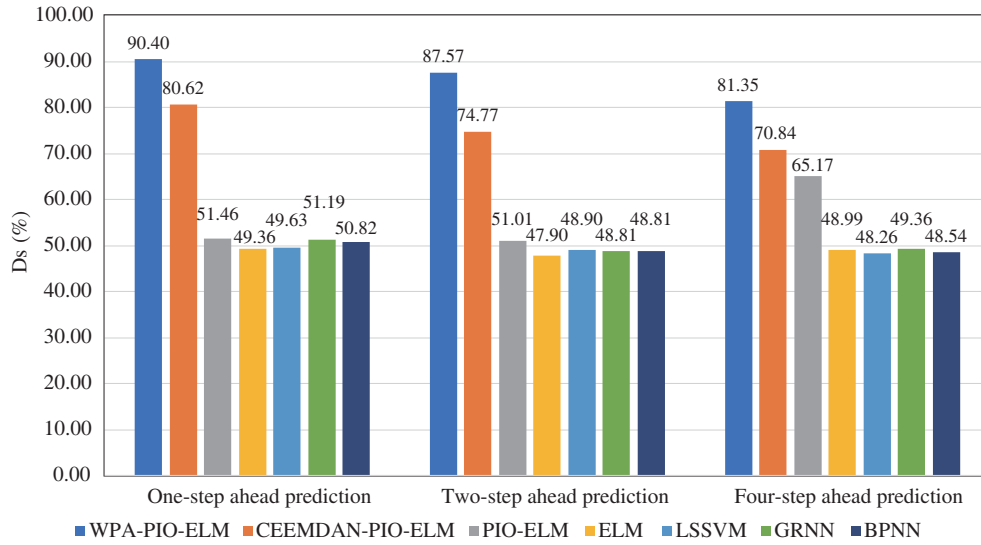


Figure 10 (Color online) Ds of WTI crude oil futures prediction.

Table 2 DM test outcomes of one-step ahead prediction of WTI crude oil futures

Benchmark model	Tested model					
	CEEMDAN-PIO-ELM	PIO-ELM	ELM	LSSVM	GRNN	BPNN
WPA-PIO-ELM	-2.6052 (0.0079)	-1.9203 (0.0337)	-3.1579 (0.0022)	-2.9443 (0.0036)	-3.3404 (0.0014)	-4.9981 (2.34e-05)
CEEMDAN-PIO-ELM		-1.8080 (0.0419)	-3.0970 (0.0025)	-2.9287 (0.0038)	-3.3293 (0.0015)	-4.9979 (2.34e-05)
PIO-ELM			-2.0356 (0.0267)	-2.6472 (0.0072)	-3.1379 (0.0023)	-4.9968 (2.35e-05)
ELM				-1.7475 (0.0470)	-2.5949 (0.0081)	-4.9927 (2.38e-05)
LSSVM					-3.8140 (0.0004)	-4.9817 (2.44e-05)
GRNN						-4.9730 (2.49e-05)

tested models. If the p -value is less than 0.05, the benchmark model will have better predictive ability than the tested model. According to the results of DM statistical tests, the following conclusions can be drawn as below: (1) The outcomes of DM statistical tests are nearly the same as the error analysis results, and the forecasting precision of WPA-PIO-ELM is higher than that of other comparison models. However, for the two-step ahead prediction, the p -value between WPA-PIO-ELM and CEEMDAN-PIO-ELM is 0.1243, which is greater than 0.05. Considering the outcomes of error analysis, the proposed hybrid model is still superior to CEEMDAN-PIO-ELM. It can be seen that using WPA can effectively reduce the forecasting difficulty of futures prices and greatly enhance the forecasting accuracy of the hybrid model. (2) The predictive ability of PIO-ELM is also better than ELM, which shows that PIO can improve the forecasting precision of ELM. (3) According to the results of the three types of prediction, there is no significant difference among the forecasting abilities of LSSVM, GRNN and BPNN.

3.2.2 Comparative analysis of CBOT soybean futures forecasting

The CBOT soybean futures prices are decomposed by a three-layer WPA, and Figure 11 shows the decomposition subseries of the CBOT soybean futures. The outcomes of CBOT soybean futures error analysis for one-step, two-step and four-step ahead predictions are displayed in Figures 12–17. It can illustrate the following conclusions. (1) Based on the values of MAPE, the WPA-PIO-ELM errors are

Table 3 DM test outcomes of two-step ahead prediction of WTI crude oil futures

Benchmark model	Tested model					
	CEEMDAN-PIO-ELM	PIO-ELM	ELM	LSSVM	GRNN	BPNN
WPA-PIO-ELM	-1.1835 (0.1243)	-2.3021 (0.0154)	-2.6263 (0.0075)	-5.5253 (6.40e-06)	-4.8258 (3.59e-05)	-2.4828 (0.0104)
CEEMDAN-PIO-ELM		-2.2151 (0.0185)	-2.5941 (0.0081)	-5.5220 (6.45e-06)	-4.8200 (3.65e-05)	-2.4798 (0.0105)
PIO-ELM			-1.6824 (0.0530)	-5.4803 (7.14e-06)	-4.7432 (4.41e-05)	-2.3821 (0.0129)
ELM				-5.5512 (6.01e-06)	-4.8177 (3.67e-05)	-2.3426 (0.0141)
LSSVM					6.2658 (1.0000)	4.5846 (0.9999)
GRNN						1.5720 (0.9352)

Table 4 DM test outcomes of four-step ahead prediction of WTI crude oil futures

Benchmark model	Tested model					
	CEEMDAN-PIO-ELM	PIO-ELM	ELM	LSSVM	GRNN	BPNN
WPA-PIO-ELM	-2.1870 (0.0196)	-2.6353 (0.0074)	-3.3719 (0.0013)	-5.4831 (7.094e-06)	-4.8650 (3.26e-05)	-2.2768 (0.0162)
CEEMDAN-PIO-ELM		-2.5505 (0.0089)	-3.3183 (0.0015)	-5.4777 (7.189e-06)	-4.8556 (3.337e-05)	-2.1432 (0.0215)
PIO-ELM			-2.3883 (0.0128)	-5.4729 (7.272e-06)	-4.8288 (3.568e-05)	0.4089 (0.6568)
ELM				-5.5533 (5.976e-06)	-4.8777 (3.159e-05)	2.8062 (0.9950)
LSSVM					6.2270 (1.0000)	5.4896 (1.0000)
GRNN						1.5720 (1.0000)

Table 5 PT test outcomes of WTI crude oil futures prediction

	WPA-PIO-ELM	CEEMDAN-PIO-ELM	PIO-ELM	ELM	LSSVM	GRNN	BPNN
One-step ahead prediction	45.4319 (0.0000)	25.6441 (0.0000)	0.9511 (0.3416)	-0.5960 (0.5512)	-0.2667 (0.7897)	0.7757 (0.4379)	0.4879 (0.6256)
Two-step ahead prediction	37.7136 (0.0000)	18.8974 (0.0000)	0.6604 (0.5090)	-1.4355 (0.1511)	-0.7289 (0.4661)	-0.7529 (0.4515)	-0.7486 (0.4541)
Four-step ahead prediction	26.6502 (0.0000)	15.1759 (0.0000)	-0.7426 (0.4577)	-0.7186 (0.4724)	-1.2499 (0.2113)	-0.3596 (0.7191)	-0.9909 (0.3217)

close to 0, and the minimum value of the three types of the prediction is 0.11%. Compared to the PIO-ELM model, the prediction errors of the WPA-PIO-ELM method are reduced by 88.20%, 76.60% and 77.05%, respectively. The forecasting errors of PIO-ELM are lower 30.53%, 18.45% and 20.35% than ELM respectively. Hence, the proposed hybrid model can improve the prediction performance of bulk commodity futures prices. (2) NRMSE and TIC are two types of indices for evaluating RMSE. The values of TIC are all less than 0.04 and the values of NRMSE are all less than 11%, which can indicate that the seven models have better forecasting performance based on the two indicators. (3) IA is a dimensionless index, and the values of WPA-PIO-ELM reach its upper limit. It can indicate that the hybrid-forecasting model is effective in predicting the prices of CBOT soybean futures. (4) BPNN has the poorest performance among the forecasting models. For predicting CBOT soybean futures, the forecasting performances of GRNN and LSSVM are similar to each other, which are both less accurate

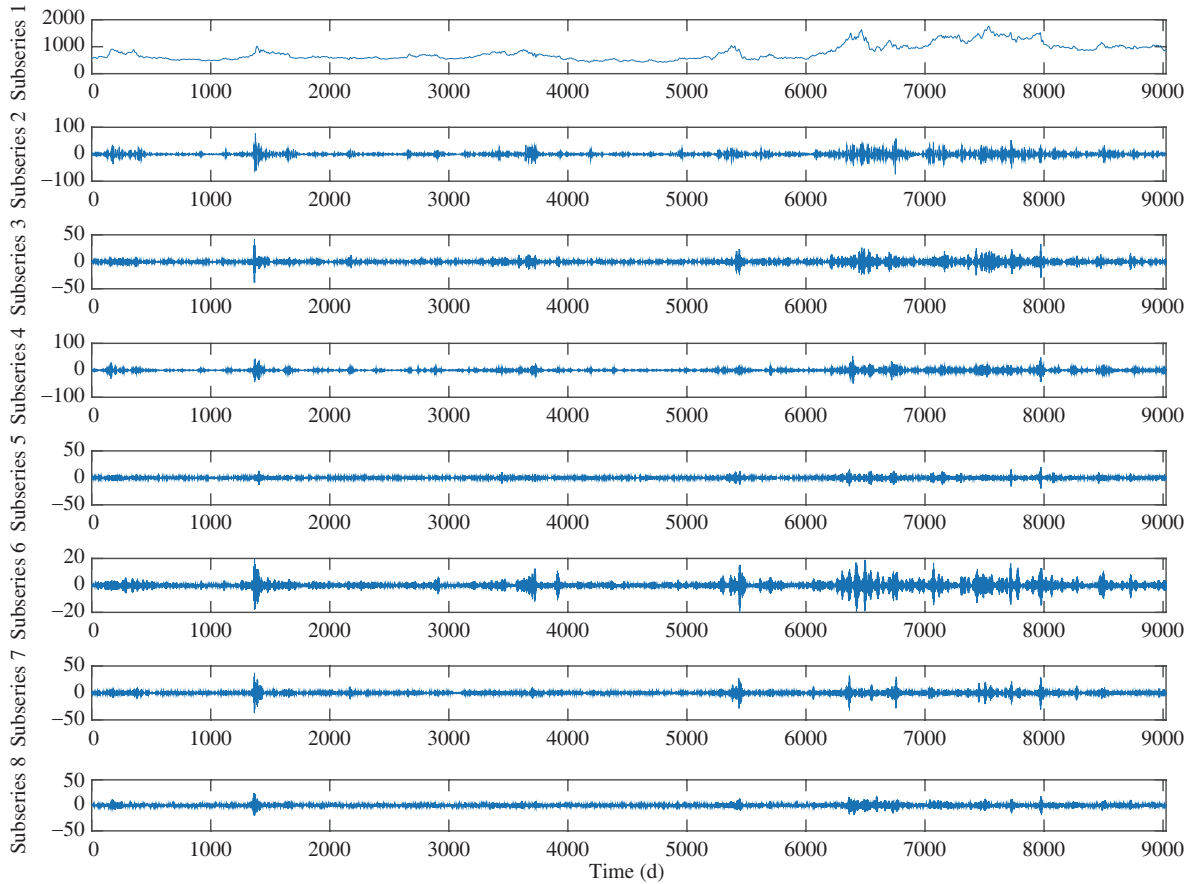


Figure 11 (Color online) Decomposition of CBOT soybean futures prices.

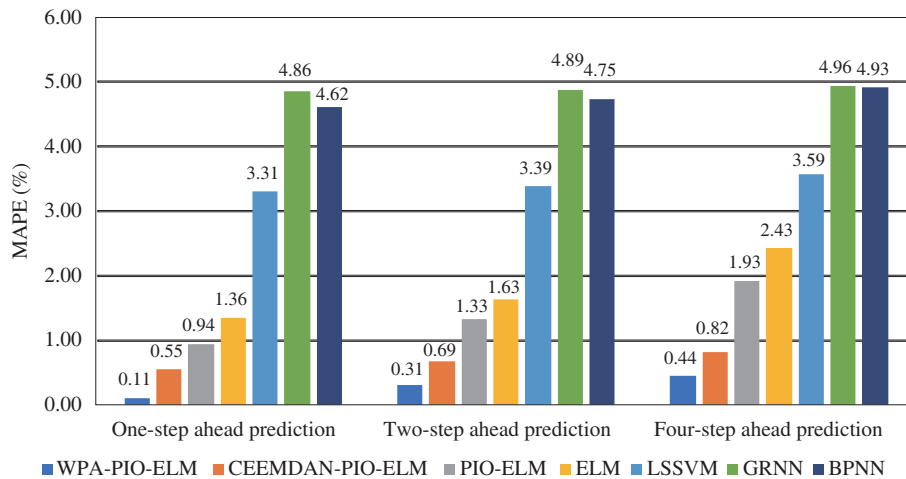


Figure 12 (Color online) MAPE of CBOT soybean futures prediction.

than ELM.

Tables 6–9 display the DM and PT test results for one-step, two-step and four-step ahead predictions. The hybrid WPA-PIO-ELM and CEEMDAN-PIO-ELM models are more accurate than the other single models. Decomposition approaches can enhance the precision of the original models from two perspectives of horizon and direction. The forecasting abilities of GRNN, BPNN and LSSVM are very similar according to the DM and PT test outcomes, and ELM is the best model for forecasting the futures prices of bulk commodities among the four single approaches.

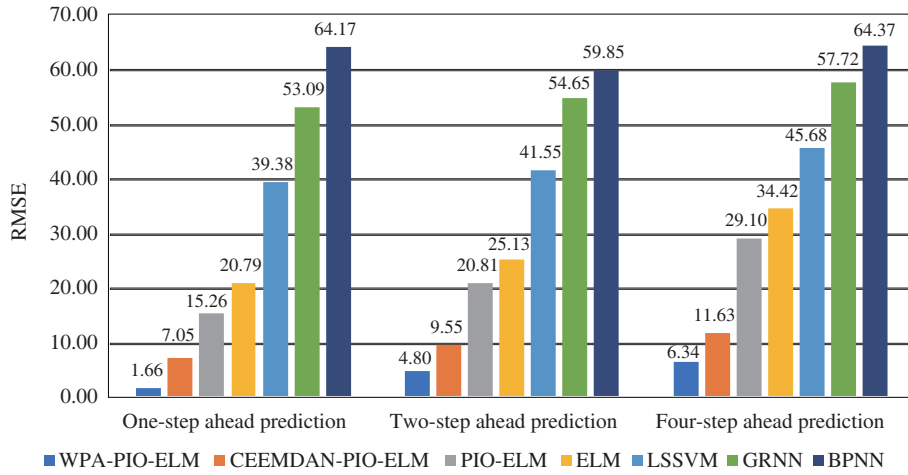


Figure 13 (Color online) RMSE of CBOY soybean futures prediction.

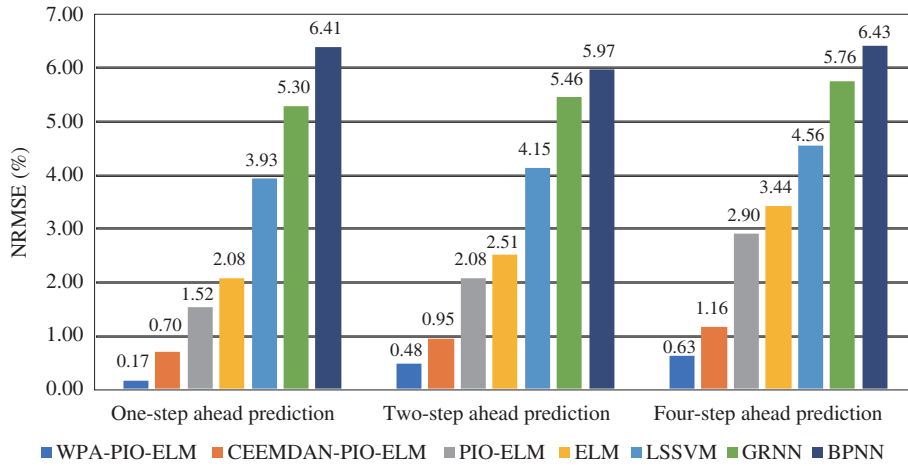


Figure 14 (Color online) NRMSE of CBOY soybean futures prediction.

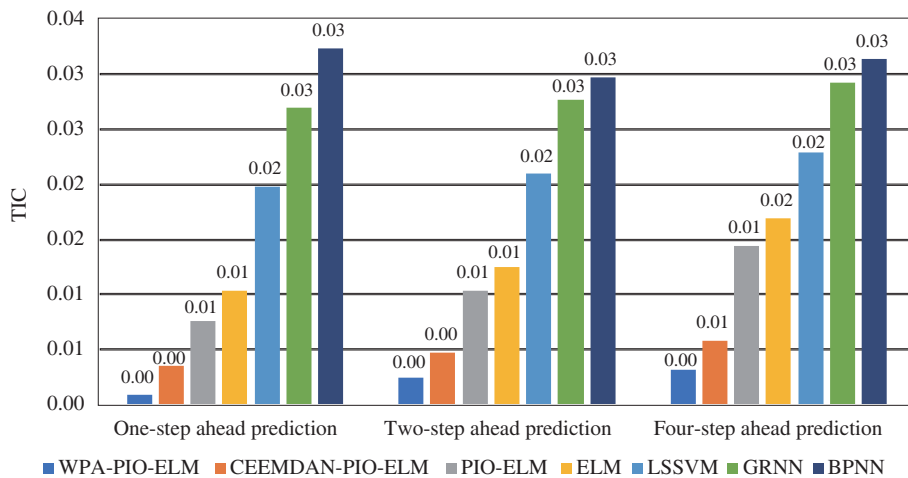


Figure 15 (Color online) TIC of CBOY soybean futures prediction.

3.3 Robustness analysis

In this subsection, we further examine the robustness of the proposed hybrid-forecasting model from two different perspectives. First, we run the models twenty times. Owing to the fact that NRMSE and TIC

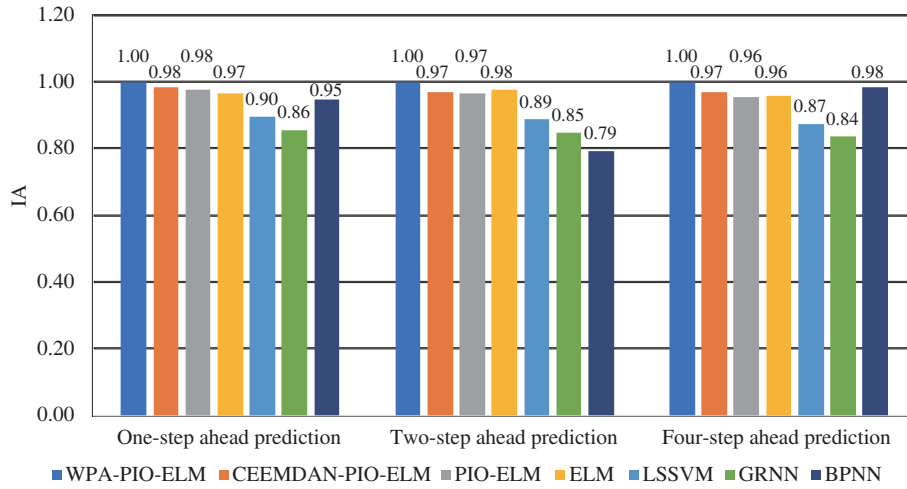


Figure 16 (Color online) IA of CBOT soybean futures prediction.

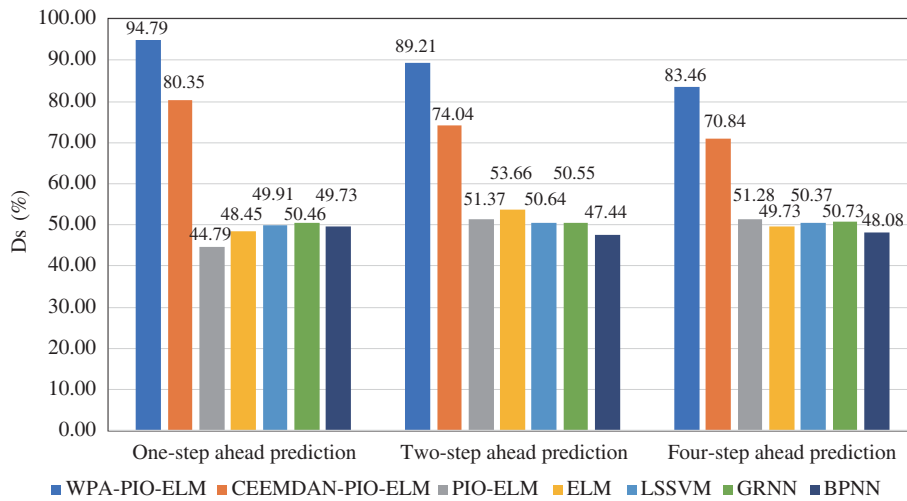


Figure 17 (Color online) Ds of CBOT soybean futures prediction.

Table 6 DM test outcomes of one-step ahead prediction of CBOT soybean futures

Benchmark model	Tested model					
	CEEMDAN-PIO-ELM	PIO-ELM	ELM	LSSVM	GRNN	BPNN
WPA-PIO-ELM	-2.0316 (0.0270)	-1.3856 (0.0896)	-2.1278 (0.0222)	-4.8871 (3.09e-05)	-5.4659 (7.40e-06)	-3.0946 (0.0026)
CEEMDAN-PIO-ELM		-1.3097 (0.1016)	-2.0564 (0.0256)	-4.8841 (3.11e-05)	-5.4644 (7.43e-06)	-3.0944 (0.0026)
PIO-ELM			-2.2538 (0.0170)	-4.7482 (4.36e-05)	-5.3783 (9.17e-06)	-3.0891 (0.0026)
ELM				-4.7634 (4.20e-05)	-5.3927 (8.85e-06)	-3.0884 (0.0026)
LSSVM					-6.2995 (9.95e-07)	-2.8916 (0.0041)
GRNN						-2.6876 (0.0066)

are two evaluation indices of RMSE, we only calculate the standard deviations of the MAPE, RMSE, IA and Ds results. A smaller standard deviation indicates better robustness. Second, the prices of natural

Table 7 DM test outcomes of two-step ahead prediction of CBOT soybean futures

Benchmark model	Tested model					
	CEEMDAN-PIO-ELM	PIO-ELM	ELM	LSSVM	GRNN	BPNN
WPA-PIO-ELM	-2.4016 (0.0124)	-2.3861 (0.0128)	-1.9301 (0.0330)	-5.0574 (2.02e-05)	-5.6073 (5.24e-06)	-1.9580 (0.0312)
CEEMDAN-PIO-ELM		-2.3263 (0.0146)	-1.9052 (0.0347)	-5.0528 (2.05e-05)	-5.6045 (5.28e-06)	-1.9345 (0.0327)
PIO-ELM			-0.4727 (0.3205)	-4.8624 (3.28e-05)	-5.4854 (7.05e-06)	-0.9618 (0.1731)
ELM				-5.1623 (1.56e-05)	-5.7208 (3.98e-06)	-0.6101 (0.2739)
LSSVM					-6.4966 (6.26e-07)	4.3509 (0.9999)
GRNN						5.1468 (1.0000)

Table 8 DM test outcomes of four-step ahead prediction of CBOT soybean futures

Benchmark model	Tested model					
	CEEMDAN-PIO-ELM	PIO-ELM	ELM	LSSVM	GRNN	BPNN
WPA-PIO-ELM	-2.3803 (0.0130)	-3.3016 (0.0016)	-1.8914 (0.0356)	-5.7202 (3.98e-06)	-6.2204 (1.20e-06)	-4.7718 (4.11e-05)
CEEMDAN-PIO-ELM		-3.1817 (0.0021)	-1.8754 (0.0368)	-5.7113 (4.07e-06)	-6.2153 (1.21e-06)	-4.7581 (4.25e-05)
PIO-ELM			-1.5243 (0.0705)	-5.5971 (5.37e-06)	-6.1524 (1.41e-06)	-4.6515 (5.55e-05)
ELM				-5.8226 (3.11e-06)	-6.6770 (4.11e-07)	-4.2913 (0.0001)
LSSVM					-7.1382 (1.43e-07)	-1.2593 (0.1103)
GRNN						1.3198 (0.9001)

Table 9 PT test outcomes of CBOT soybean futures prediction

	WPA-PIO-ELM	CEEMDAN-PIO-ELM	PIO-ELM	ELM	LSSVM	GRNN	BPNN
One-step ahead prediction	67.4621 (0.0000)	25.4103 (0.0000)	-2.8837 (0.0039)	-0.6938 (0.4878)	-4.0953 (4.2162e-05)	-3.8716 (0.0001)	-2.7188 (0.0066)
Two-step ahead prediction	42.0257 (0.0000)	18.2267 (0.0000)	1.1240 (0.2610)	2.9933 (0.0028)	-2.2243 (0.0261)	-3.4929 (0.0005)	-2.0437 (0.0410)
Four-step ahead prediction	29.9611 (0.0000)	15.2254 (0.0000)	1.0903 (0.2756)	0.6843 (0.4938)	-1.7956 (0.0726)	-2.5590 (0.0105)	0.0678 (0.9459)

gas futures of New York commodity exchange and gold futures of Chicago commodity futures exchange, which are obtained from US Energy Information Administration and Wind database, are adopted to make the analysis of robustness. We perform the same prediction by using the proposed WPA-PIO-ELM model. Tables 10 and 11 show the robustness analysis outcomes of WTI crude oil futures and CBOT soybean futures. Table 12 displays the forecasting errors of natural gas and gold futures for one-step, two-step and four-step ahead predictions.

The above tables demonstrate that the robustness of the WPA-PIO-ELM is superior among the predictive models. The robustness of LSSVM is better than that of GRNN and BPNN, whereas the robustness of BPNN is the poorest among the seven models. The two decomposition algorithms and the PIO algorithm have greatly improved the robustness of the ELM. By adopting the prices of natural gas futures and gold futures for one-step, two-step and four-step ahead predictions, it can be find that the horizontal

Table 10 Robustness analysis of WTI crude oil futures prediction

WTI forecasting	Standard deviation	WPA-PIO-ELM	CEEMDAN-PIO-ELM	PIO-ELM	ELM	LSSVM	GRNN	BPNN
One-step ahead prediction	MAPE	0.0023	0.0033	0.0041	0.0274	0.4093	0.2818	1.1207
	RMSE	0.0007	0.0006	0.0005	0.0185	0.2896	0.1956	0.5645
	IA	0.0005	0.0005	0.0005	0.0009	0.0025	0.0021	0.0165
	Ds	0.6398	0.5829	0.5941	0.9787	1.1890	0.6727	0.9041
Two-step ahead prediction	MAPE	0.0033	0.0060	0.0073	0.0062	0.3667	0.2453	1.8952
	RMSE	0.0011	0.0009	0.0001	0.0040	0.2619	0.1745	1.1927
	IA	0.0001	0.0002	0.0002	0.0001	0.0030	0.0022	0.0263
	Ds	0.3200	0.3017	0.3200	0.3219	0.1882	0.8019	0.6411
Four-step ahead prediction	MAPE	0.0064	0.0082	0.0146	0.0067	0.2408	0.7800	0.6390
	RMSE	0.0142	0.0034	0.0029	0.0142	0.1709	0.1746	0.3951
	IA	0.0006	0.0003	0.0003	0.0003	0.0034	0.0053	0.0017
	Ds	0.0457	0.1371	0.1828	0.3206	0.4767	0.3535	1.2520

Table 11 Robustness analysis of CBOT soybean futures prediction

WTI forecasting	Standard deviation	WPA-PIO-ELM	CEEMDAN-PIO-ELM	PIO-ELM	ELM	LSSVM	GRNN	BPNN
One-step ahead prediction	MAPE	0.0016	0.0027	0.0035	0.0425	0.1370	0.1668	0.5557
	RMSE	0.0043	0.0049	0.0043	0.5918	1.7537	2.1322	6.9070
	IA	0.0003	0.0004	0.0003	0.0012	0.0186	0.0109	0.0331
	Ds	0.3656	0.8311	0.3656	0.8799	2.2887	0.6377	2.3280
Two-step ahead prediction	MAPE	0.0014	0.0048	0.0061	0.0841	0.1234	0.0882	0.8240
	RMSE	0.0142	0.0379	0.0236	0.9338	1.6310	1.0437	7.9131
	IA	0.0007	0.0008	0.0007	0.0023	0.0121	0.0107	0.0192
	Ds	0.4570	0.5484	0.0914	0.8585	0.6717	0.7550	1.8164
Four-step ahead prediction	MAPE	0.0011	0.0035	0.0030	0.0482	0.2231	0.0690	0.1893
	RMSE	0.0147	0.0122	0.0092	0.5842	2.0020	0.9416	2.4118
	IA	0.0004	0.0004	0.0001	0.0017	0.0357	0.0221	0.0151
	Ds	0.2286	0.1975	0.0457	0.1293	0.6463	1.1003	1.7166

Table 12 Forecasting errors of natural gas futures and gold futures

	Statistical indicator	Nature gas futures prediction	Gold futures prediction
One-step ahead prediction	MAPE (%)	0.1116	0.037
	RMSE	0.0043	0.5987
	NRMSE (%)	0.1424	0.0482
	TIC	6.95e-04	2.41e-04
	IA	1.0000	0.9981
	Ds (%)	97.532	97.8976
Two-step ahead prediction	MAPE (%)	0.2781	0.1027
	RMSE	0.0109	1.6174
	NRMSE (%)	0.3638	0.1303
	TIC	0.0018	6.51e-04
	IA	0.9999	0.9975
	Ds (%)	94.6069	94.4241
Four-step ahead prediction	MAPE (%)	0.7844	0.3637
	RMSE	0.0303	5.8779
	NRMSE (%)	1.0091	0.4737
	TIC	0.0049	0.0024
	IA	1.0000	0.9816
	Ds (%)	86.4717	81.8099

prediction errors of the hybrid WPA-PIO-ELM models are close to 0 and the values of Ds are all above 80%.

Table 13 Forecasting errors of SSA-K-means-ELM

	Statistical indicator	WTI crude oil futures prediction	CBOT soybean futures prediction
One-step ahead prediction	MAPE (%)	1.1215	0.6760
	RMSE	0.7707	10.5351
	NRMSE (%)	1.3259	1.0516
	TIC	0.0063	0.0052
	IA	0.9974	0.9846
	Ds (%)	75.5027	75.3199
Two-step ahead prediction	MAPE (%)	1.3259	0.6601
	RMSE	0.7616	10.3798
	NRMSE (%)	1.3104	1.0361
	TIC	0.0062	0.0051
	IA	0.9979	0.9830
	Ds (%)	76.3254	75.5941
Four-step ahead prediction	MAPE (%)	1.2198	0.7177
	RMSE	0.8328	11.1091
	NRMSE (%)	1.4329	1.1089
	TIC	0.0068	0.0055
	IA	0.9947	0.9661
	Ds (%)	72.8519	73.5832

Table 14 Forecasting errors of EMD-RBF

	Statistical indicator	WTI crude oil futures prediction	CBOT soybean futures prediction
One-step ahead prediction	MAPE (%)	1.3284	0.5209
	RMSE	1.5300	10.1198
	NRMSE (%)	2.6246	1.0102
	TIC	0.0125	0.0050
	IA	0.9992	0.9994
	Ds (%)	78.6106	83.9122
Two-step ahead prediction	MAPE (%)	1.6458	0.6556
	RMSE	2.1256	9.9750
	NRMSE (%)	3.6478	0.9957
	TIC	0.0174	0.0049
	IA	0.9908	0.9927
	Ds (%)	77.0567	78.9762
Four-step ahead prediction	MAPE (%)	3.1846	0.7993
	RMSE	2.6471	12.3883
	NRMSE (%)	4.5502	1.2366
	TIC	0.0216	0.0061
	IA	0.9940	0.9944
	Ds (%)	70.2393	73.2176

3.4 Discussion

For verifying the superiority of the WPA-PIO-ELM model proposed in this paper, we make comparisons with the methods in [23,24]. Wang et al. [23] developed a hybrid SSA-K-means-ELM model to predict the prices of bulk commodity futures, and Lu [24] proposed a hybrid EMD-RBF to forecast stock index futures prices. We utilize the SSA-K-means-ELM and EMD-RBF models to forecast the prices of WTI crude oil and CBOT soybean futures respectively. The results of error analysis of the SSA-K-means-ELM and EMD-RBF models are shown in Tables 13 and 14. According to the error analysis of the two models, it reveals that the proposed WPA-PIO-ELM model has better performance than that of the SSA-K-means-ELM and EMD-RBF models. The best Ds values of the two comparison models are 76.33% and 83.91% and the best Ds value of the proposed WPA-PIO-ELM model can reach 94.79%. Therefore, the proposed

hybrid-forecasting model exhibits a better performance on directional estimation. In terms of horizontal accuracy, the prediction errors of the WPA-PIO-ELM model are less than those of the comparison models. Hence, it can be found that the PIO algorithm can improve the forecasting precision of ELM and WPA is much fitter than SSA and EMD in decomposing the futures prices of bulk commodities. Based on the results of error analysis, statistical tests, robustness analysis and comparative outcomes, we can draw three conclusions as follows. (1) The proposed WPA-PIO-ELM model is remarkably superior to other comparison models, which has better horizontal precision, directional precision and robustness in predicting bulk commodity futures prices. (2) ELM has better performance on bulk commodity futures prices than that of other single models, and PIO can effectively optimize the parameters of ELM and improve its forecasting accuracy. (3) The WPA decomposition method has a superior decomposition ability than EMD, CEEMDAN and SSA, and it can greatly reduce the forecasting difficulty and make the hybrid WPA-PIO-ELM model predict futures prices more accurately.

4 Conclusion

In this paper, we proposed a hybrid approach of PIO and ELM based on WPA to predict bulk commodity futures prices. This hybrid WPA-PIO-ELM forecasting model effectively improved the estimation accuracy of bulk commodity futures prices. WPA is employed to decompose the original futures prices into a set of subseries, which can reduce the volatility and prediction difficulty of the initial data. PIO is used to optimize the initial weights and thresholds of ELM, and the improved ELM is adopted to predict the price series of bulk commodity futures. For testing the superiority of the hybrid WPA-PIO-ELM model, we utilized a series of WTI crude oil futures, CBOT soybean futures, natural gas futures and gold futures prices to make one-step, two-step and four-step ahead predictions. The proposed hybrid-forecasting model has excellent performance on bulk commodity futures price estimation. It also has better performance in horizontal precision, directional precision and robustness. In future work, we plan to integrate PIO with other intelligent algorithms and further enhance the optimization ability of PIO. We will then utilize the improved hybrid model to solve more complicated industrial and financial problems.

Acknowledgements This work was supported by National Natural Science Foundation of China (Grant Nos. 61773401, 61304067, 11601524, 61761130081) and Foundation of Hubei Province of China (Grant Nos. 17G024, 2017132).

References

- 1 Chi G T, Li Z J. Forecast model of stock index futures prices based on small sample. *ICIC Express Lett Part B Appl Int J Res Surv*, 2014, 5: 657–662
- 2 Wang C Y. Forecast on price of agricultural futures in China based on ARIMA model. *Asian Agr Res*, 2016, 8: 9–12
- 3 Darekar A, Reddy A. Predicting market price of soybean in major india studies through ARIMA model. *Soc Sci Electron Publishing*, 2017, 30: 73–76
- 4 Xu W C, Zhou H B, Cheng N, et al. Internet of vehicles in big data era. *IEEE/CAA J Autom Sin*, 2018, 5: 19–35
- 5 Mazouchi M, Naghibi-Sistani M B, Sani S K H. A novel distributed optimal adaptive control algorithm for nonlinear multi-agent differential graphical games. *IEEE/CAA J Autom Sin*, 2018, 5: 331–341
- 6 Zhang Y H, Shen X, Shen T L. A survey on online learning and optimization for spark advance control of SI engines. *Sci China Inf Sci*, 2018, 61: 070201
- 7 Li H T, Zhao G D, Meng M, et al. A survey on applications of semi-tensor product method in engineering. *Sci China Inf Sci*, 2018, 61: 010202
- 8 Baruník J, Malinská B. Forecasting the term structure of crude oil futures prices with neural networks. *Appl Energy*, 2016, 164: 366–379
- 9 Hu J W S, Hu Y C, Lin R R W. Applying neural networks to prices prediction of crude oil futures. *Math Probl Eng*, 2012, 2012: 1–12
- 10 Zhang X M, Han Q L, Zeng Z. Hierarchical type stability criteria for delayed neural networks via canonical bessel-legendre inequalities. *IEEE Trans Cybern*, 2018, 48: 1660–1671
- 11 Zhang Y, He J, Yin T F. Research on petroleum price prediction based on SVM. *Comput Simul*, 2012, 29: 375–377
- 12 Zhang J L, Zhang Y J, Zhang L. A novel hybrid method for crude oil price forecasting. *Energy Econ*, 2015, 49: 649–659
- 13 Das S P, Padhy S. A novel hybrid model using teaching-learning-based optimization and a support vector machine for commodity futures index forecasting. *Int J Mach Learn Cyber*, 2018, 9: 97–111
- 14 Ela A A A E, Abido M A, Spea S R. Differential evolution algorithm for optimal reactive power dispatch. *Electric Power Syst Res*, 2011, 81: 458–464

- 15 Zhang D F, Duan H B, Yang Y J. Active disturbance rejection control for small unmanned helicopters via Levy flight-based pigeon-inspired optimization. *Aircraft Eng Aerospace Tech*, 2017, 89: 946–952
- 16 Chen H H, Chen M, Chiu C C. The integration of artificial neural networks and text mining to forecast gold futures prices. *Commun Stat-Simul Comput*, 2016, 45: 1213–1225
- 17 Dou R, Duan H B. Pigeon inspired optimization approach to model prediction control for unmanned air vehicles. *Aircraft Eng Aerospace Tech*, 2016, 88: 108–116
- 18 Pang B, Liu M, Zhang X, et al. A novel approach framework based on statistics for reconstruction and heartrate estimation from PPG with heavy motion artifacts. *Sci China Inf Sci*, 2018, 61: 022312
- 19 Sun S L, Wang S Y, Zhang G W, et al. A decomposition-clustering-ensemble learning approach for solar radiation forecasting. *Sol Energy*, 2018, 163: 189–199
- 20 Liu H, Mi X W, Li Y F. Comparison of two new intelligent wind speed forecasting approaches based on wavelet packet decomposition, complete ensemble empirical mode decomposition with adaptive noise and artificial neural networks. *Energy Convers Manag*, 2018, 155: 188–200
- 21 Jiang F, He J Q, Zeng Z G, et al. A decomposition-optimization-ensemble learning approach for electricity price forecasting (in Chinese). *Sci Sin Inform*, 2018, 48: 1300–1315
- 22 Wang D Y, Yue C Q, Wei S, et al. Performance analysis of four decomposition-ensemble models for one-day-ahead agricultural commodity futures price forecasting. *Algorithms*, 2017, 10: 108
- 23 Wang Y, Qi C, Li M F. Prediction of commodity prices based on SSA-ELM. *Syst Eng-Theory Pract*, 2017, 37: 2004–2014
- 24 Lu H F. Price forecasting of stock index futures based on a new hybrid EMD-RBF neural network model. *Agro Food Ind Hi Tech*, 2017, 28: 1744–1747
- 25 Wang J, Li X. A combined neural network model for commodity price forecasting with SSA. *Soft Comput*, 2018, 22: 5323–5333
- 26 Huang G B, Zhu Q Y, Siew C K. Extreme learning machine: theory and applications. *Neurocomputing*, 2006, 70: 489–501
- 27 Duan H B, Qiao P X. Pigeon-inspired optimization: a new swarm intelligence optimizer for air robot path planning. *Int J Intel Comput Cyber*, 2014, 7: 24–37
- 28 Diebold F X, Mariano R S. Comparing predictive accuracy. *J Business Economic Stat*, 2002, 20: 134–144
- 29 Pesaran M H, Timmermann A. A simple nonparametric test of predictive performance. *J Business Economic Stat*, 1992, 10: 461–465
- 30 Helske J, Luukko P. Ensemble empirical mode decomposition (EEMD) and its complete variant (CEEMDAN). *Int J Public Health*, 2016, 60: 1–9